

Kinetics of exciton condensation in germanium

V. S. Bagaev, N. V. Zamkovets, L. V. Keldysh, N. N. Sibel'din, and V. A. Tsvetkov

P. N. Lebedev Physics Institute, USSR Academy of Sciences
(Submitted November 6, 1975)
Zh. Eksp. Teor. Fiz. **70**, 1501-1521 (April 1976)

A light-scattering method is used to investigate the dimension and the concentration of electron-hole drops (EHD) in germanium as functions of the temperature, excitation intensity, and waveform of the exciting light pulse. It is shown that the dependences of the condensed-phase volume on the temperature and intensity of the excitation are determined mainly by the number of produced drops (especially near the condensation threshold). It is observed that nuclei of the EHD are produced mainly when the excitation is turned on, i.e., on the front of the exciting pulse. Theoretical expressions are obtained for the description of the EHD density as a function of the temperature and of the excitation level at various rise times of the exciting-pulse front. The experimental results are discussed on the basis of a condensation theory that takes into account the surface tension of the electron-hole drop and the diffusion of the excitons to the surface of the EHD.

PACS numbers: 71.80.+j

INTRODUCTION

Since the publication of the first papers on electron-hole drops (EHD),^[1-7] many theoretical and experimental investigations were made of the properties of the electron-hole liquid. There is, however, a considerable gap in the understanding of the physical picture of the exciton condensation, a gap concerning the kinetics of the formation and growth of the EHD. In addition, some presently known experimental facts which are apparently also connected with the kinetics of condensation have not been satisfactorily explained in the literature. Foremost among these is the difference, observed by a number of workers, in the dependence of the intensity of the EHD on the excitation power and the difference in the values of the binding energies of the carriers in EHD, as determined from optical and thermal measurements.

There are a number of cited results on the kinetics of exciton condensation,^[8-14] obtained from measurements of the dependence of the volume of the liquid phase on the generation rate. These experimental data were analyzed on the basis of the equations of the condensation kinetics given in,^[7,8] and it was assumed in most of their interpretations that the EHD concentration in the crystal does not depend on the experimental conditions, but is determined by the number of condensation centers. It is possible that this is justified under certain conditions, although it was shown in^[15,16] that the EHD concentration depends strongly on the temperature and on the excitation intensity. In^[17,18], optical hysteresis of the intensity of the EHD emission was observed as well as a very sharp growth of the volume of the liquid phase near the condensation threshold with increasing generation level. A sharp growth of the liquid-phase volume was observed also in impurity-containing samples.^[9,10] These results are difficult to explain by assuming a fixed concentration of the EHD, as was noted in^[9].

In the analysis of the causes of the discrepancies between the values of the binding energies of the carriers in EHD, determined from spectral and thermal mea-

surements, account must be taken of the strong temperature dependence of the EHD concentration. Spectral measurements of the binding energy per pair of particles in the liquid phase were carried out in^[13,18-22]. It appears that the presently most reliable binding energy is 2.06 ± 0.15 meV.^[18,22] Temperature measurements^[13,17,23,24] yield values approximately 30% lower. It is possible that it is precisely the dependence of the rate of liquid-phase nucleus phase formation on the temperature which leads to this difference.

The binding energy was also determined from measurements of the EHD recombination and evaporation kinetics.^[23,25] These measurements yield approximately the same value as the temperature measurements. It should be noted in this connection that the results of studies of the recombination kinetics^[23,25,26] were reduced with the aid of kinetics equations^[7,8] that do not take into account the diffusion of the excitons towards the EHD surface, nor the surface tension of the electron-hole liquid. The contribution of the diffusion may turn out to be appreciable at large EHD radii. It is possible that failure to take this circumstance into account leads to a stronger growth of the EHD radius near the condensation temperature threshold, as observed in^[25]. Theoretical calculations^[27-30] and measurement results^[16,31] show that the surface-tension coefficient of the electron-hole liquid is quite high ($\sim 10^{-4}$ dyn/cm), and therefore the role of the surface tension can become noticeable at small drop radii. In^[32], the influence of surface tension on the kinetics of exciton condensation was considered, but the exciton diffusion was not taken into account there, too.

We used a light-scattering method to investigate the dependence of the dimension and concentration of the EHD in the case of volume quasistationary optical excitation on the following experimental conditions: the temperature, the excitation intensity, and the waveform of the light pulse. Our results show that the concentration of the EHD in the crystal increases with increasing excitation level and with decreasing temperature, and near the threshold temperature the dependence of the drop concentration on the generation level

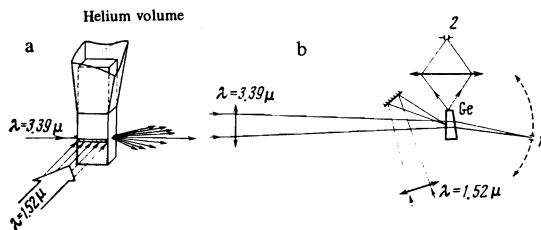


FIG. 1. System for the superposition of the laser beams in the measurement of the concentration (a) and of the total number of EHD (b): 1) entrance diaphragm of the quantum amplifier, 2) monochromator slit.

is stronger. Hysteresis-type phenomena were observed, i. e., under quasi-stationary excitation, the drop concentration increased with increasing slope of the light-pulse front.

The experimental results show that at low temperatures the stationary dimensions of the EHD are determined by the generation level and by the drop concentration. At high temperatures, when the recombination in the system comprising the exciton gas and the EHD proceeds mainly via the gas phase, the radius of the drops depends little on the excitation level and is independent of their concentration.

We have considered theoretically the model of liquid-phase nuclei formation and of their growth to form drops of stationary dimension; this model takes into account the surface tension of the electron-hole liquid and the diffusion of the excitons to the EHD drop. The presence of surface energy brings about a situation wherein EHD with radii not smaller than a certain temperature-dependent value can be in stable equilibrium with the exciton gas. This model agrees satisfactorily with experiment at low temperatures, but the behavior of the EHD radius in the high-temperature region still lacks an unambiguous explanation. Examination of the kinetics of formation of liquid-phase nuclei at various excitation conditions has made it possible to obtain for the dependence of the EHD concentration in the crystal on the temperature and on the generation levels expressions that describe correctly the experimental results.

EXPERIMENTAL PROCEDURE

The measurements were performed with a setup described in detail in^[33]. The excitation source was a helium-neon laser of ~ 10 mW power, operating at a wavelength 1.52μ . In the measurements we used two schemes for focusing the exciting radiation: in the measurements of the drop concentration, the exciting radiation was focused by a cylindrical lens on the lateral surface of the sample into a narrow strip (Fig. 1a), and in the measurement of the total number of the scattering particles it was focused on the front face of the crystal into a spot of $\sim 200 \mu$ diameter (Fig. 1b). The exciting radiation was modulated with a mechanical chopper of frequency 1 kHz. In the case when a large slope of the fronts of the exciting light pulse was required, the laser radiation was sharply focused on the modulator disk.

We investigated the scattering of $3.39\text{-}\mu$ radiation from a helium-neon laser. The beam from this laser was focused with a long-focus lens on the front surface of the crystal in the measurements in accordance with the scheme of Fig. 1a, or on the entrance diaphragm of a quantum amplifier (Fig. 1b). The beams of both lasers were collocated in accordance with the maximum of the absorption signal, and during the measurement of the total number of the drops their collocation was also monitored against the symmetry of the diffraction pattern produced when the $3.39\text{-}\mu$ radiation was diffracted by the region occupied by the EHD.^[34]

The radiation scattered by the EHD was amplified with an optical quantum amplifier operating with a helium-neon mixture and was registered with a PbS receiver cooled to $\sim 100^\circ\text{K}$. The angular distribution of the intensity of the scattered light was recorded on the chart of an automatic plotter.

Simultaneously with the scattering, we record the spectrum of the recombination radiation of germanium. To observe the photoluminescence we used a standard setup containing a high-transmission MDR-2 monochromator. The radiation was registered with a cooled PbS photoresistor.

The measurements were performed on germanium samples with residual-impurity content not larger than 10^{12} cm^{-3} . The samples measured $15 \times 5 \times 2$ mm and were sealed into the helium volume of the cryostat in such a way that the working half of the sample was in vacuum. The samples were mechanically polished, and the plane of the surface from which the scattered radiation emerged was inclined 2° to the opposite plane, in order to eliminate parasitic interference.

RESULTS AND DISCUSSION

The main results of our experiments are shown in Figs. 2–10. Although all the measurements were performed under conditions close to stationary (long-duration exciting pulses), phenomena of the hysteresis type were observed, i. e., a dependence of the result on the slope of the excitation-pulse front. We shall report first the results obtained under conditions closest to quasi-stationary, when the buildup of the excitation was quite slow (rise time $t_0 \approx 100 \mu\text{sec}$, much longer than the lifetime of either the excitons or the EHD).

Figure 2 shows the temperature dependences of the intensities I_{exc} (at the maximum of the spectral line) of the recombination radiation of the free excitons and I_d , of the EHD and also I_{abs} and I_{sc} , of the absorption and scattering signals respectively (I_{sc} is the light flux scattered at an angle 8° (in vacuum) into the aperture of the receiving system). It is seen that when the threshold temperature is reached ($T_c \approx 3.55^\circ\text{K}$ at the employed excitation level), scattering and drop-luminescence signals appear simultaneously and the absorption signal begins to grow rapidly.

Figure 3 (upper curve) and Fig. 4 (lower curve) show plots of the EHD radius and of the EHD concentration against the temperature at a fixed excitation level.

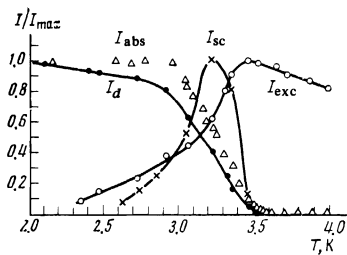


FIG. 2. Temperature dependences of absorption and scattering signals and of the intensities of the recombination radiation of the EHD and of the free excitons (the curves are normalized to their maximum values).

These measurements are performed with the beams superimposed in accordance with the scheme of Fig. 1a, and the EHD concentration was calculated from the measured values of their radii and from the magnitude of the scattering and absorption signals, as described in^[35]. The most characteristic feature of these results is the strong increase of the EHD concentration and the decrease of their radius with decreasing temperature. We note also that the angular dependence of the scattering signal agrees well with the assumption that the radii of all the observed drops are practically the same, although the limitations of the measurement procedure do not exclude a possibility of the presence in the sample of a certain amount of EHD with dimensions much larger or much smaller than those observed.

The EHD dimensions were practically independent of the distance to the illuminated surface of the sample, although the volume of the liquid phase (which is proportional to the absorption signal) decreased with increasing distance (Fig. 5). When this distance was increased from 0.5 to 1.5 mm, the EHD dimensions decreased by not more than 10–15%, and this decrease was larger at lower temperatures. Consequently, the decrease of the volume of the liquid phase with increasing distance from the illuminated surface at high temperatures (curve 3 of Fig. 5) is more readily connected with a decrease of the drop concentration. In^[36], a stronger change in the drop dimension with depth was observed. It is possible that this discrepancy is due to the fact that when an incandescent lamp is used as an excitation source the distribution of the nonequilibrium carriers bound in the EHD over the thickness of the sample is relatively inhomogeneous even at low

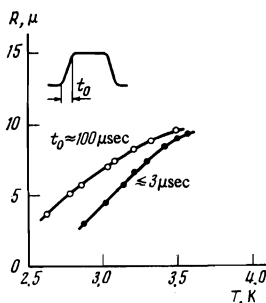


FIG. 3. Temperature dependences of EHD radius, measured using exciting pulses with long and short fronts. In the upper left corner is shown the wave form of the exciting pulse.

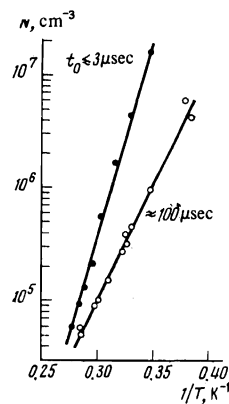


FIG. 4. Temperature dependences of the EHD concentration for long and short exciting-pulse fronts.

temperatures.

The measurement setup illustrated in Fig. 1a is the most convenient for the interpretation of the data on light scattering by EHD. However, the power of the employed excitation source in this geometry of the excited region made it possible to produce only relatively low concentrations of impurity carriers, so that the threshold condensation temperature in the experiments described above did not exceed 3.55 °K, and furthermore, it was impossible to trace the dependences of the concentration and of the EHD dimensions on the excitation level.

To investigate these dependences in the most interesting temperature region, 2.5 °K ≤ T ≤ 4.2 °K, the beams were superimposed in accordance with the scheme of Fig. 1b with relatively sharp focusing of the exciting beam. Then, however, the scattering experiments determine not the EHD concentration, but the total number of the drops along the path of the probing beam, which varies with changing temperature and with changing excitation level not in proportion to the concentration, inasmuch as the spatial distribution of the EHD over the depth of the sample changes (Fig. 5). Therefore the EHD concentration (N , in relative units) was calculated as the ratio of the intensity of the recombination radiation of the EHD to the cube of the EHD radius (the monochromator slit cut out a strip of width ≈ 0.3 mm near the illuminated surface of the sample). The absolute values of the total number of electron-hole pairs and of the total number of EHD in

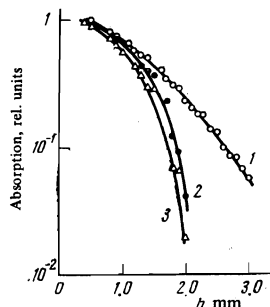


FIG. 5. Distribution of the absorption over the sample thickness: 1) $T=2.8$ °K, $P=8$ mW; 2) $T=2.8$ °K, $P=2.4$ mW; 3) $T=3.8$ °K, $P=8$ mW (P is the power of a laser with wavelength 1.52 μ, h is the distance from the illuminated surface.)

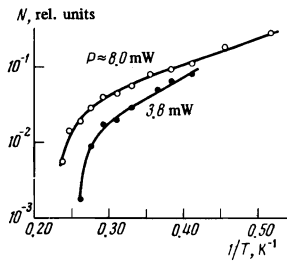


FIG. 6. Temperature dependences of the EHD concentration at two different excitation intensities. Front duration $t_0 \approx 100 \mu \text{ sec}$.

the sample at the maximum excitation level, estimated from measurements of the absorption scattering, were respectively $\sim 10^{12}$ and $\sim 10^4$ at 1.9°K , and their concentrations were $\sim 2 \times 10^{15}$ and $\sim 2 \times 10^7 \text{ cm}^{-3}$.

It is seen from Fig. 6 that the very sharp growth of the EHD concentration with decreasing temperature, observed at $T \gtrsim 3^\circ \text{K}$, slows down greatly at lower temperatures. The growth of the EHD concentration with increasing excitation level g also slows down with decreasing temperature (Fig. 7a). The $N(g)$ dependence is superlinear at temperatures relatively close to the threshold, and sublinear at $T \lesssim 3^\circ \text{K}$.

We note finally one more striking result (Fig. 8): at temperatures $T \gtrsim 3^\circ \text{K}$ the EHD radii are equal to $\approx 10 \mu$ and are practically independent of either the temperature or the excitation level.

So far we have described the results obtained with a slow (quasi-stationary) growth of the light intensity in the exciting pulses. The results of experiments in which the sample was excited with pulses of practically the same duration ($\sim 500 \mu \text{ sec}$) but with much shorter rise times ($t_0 \lesssim 3 \mu \text{ sec}$) are shown in Fig. 3 (lower curve), Fig. 4 (upper curve), and in Figs. 7b, 9, and 10. Although practically all the general tendencies remain the same as before, it is seen from these figures that given the temperature and the excitation level, the EHD concentration is higher, and their radius is smaller, than in the case of excitation with smoothly growing pulses. In addition, the EHD concentration increases more rapidly with decreasing temperature and with increasing excitation level. The function $N(g)$ turns out to be significantly superlinear (Fig. 7b) in the entire temperature interval ($T \gtrsim 2.5^\circ \text{K}$). This ex-

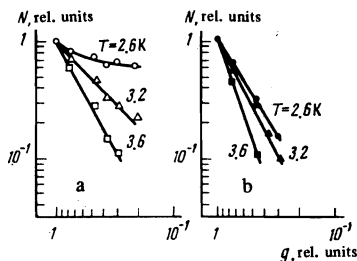


FIG. 7. Dependence of the EHD concentration on the excitation level at three different temperatures: a) $t_0 \approx 100 \mu \text{ sec}$, b) $t_0 \lesssim 3 \mu \text{ sec}$.

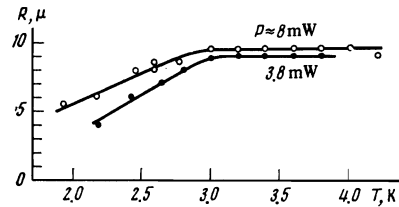


FIG. 8. Temperature dependence of the EHD radius at two different excitation intensities ($t_0 \approx 100 \mu \text{ sec}$).

plains, in particular, the only qualitative difference between the results obtained using exciting pulses with long and short pulses, i. e., the directly contradictory dependences of the EHD radii on the excitation level, namely, when the exciting pulse has a long rise time the radius increases with increasing excitation level (Fig. 8), and in the case of a short rise time it decreases (Fig. 10). We emphasize that at temperatures $T \gtrsim 3.5^\circ \text{K}$ the EHD radius tends to the same value ($\sim 10 \mu$) as in the case of a long rise time of the exciting light pulse.

As will be shown below, all these differences can be explained in the following manner: When the exciting pulses have short rise times, a strongly supersaturated exciton "vapor" is produced in the sample within a short time, as a result of which a large number of EHD nuclei begin to grow practically simultaneously. On the other hand in the case of a slow rise of the excitation, the relatively small number of EHD that begin to grow ahead of the others manage to absorb all the excess of the subsequently introduced nonequilibrium carriers, preventing by the same token the formation of new drops.

An analysis of the kinetics of the formation of the condensates calls for a consideration of two essentially different questions: the onset of the EHD nuclei and the growth of each individual drop until equilibrium is established between it and the surrounding exciton gas. We start with the second of these problems, since it is simpler.

The change in the number of particles in a spherical drop of radius R is determined by the equation

$$\frac{d}{dt} \left(\frac{4}{3} \pi R^3 n_0 \right) = S - \frac{4}{3} \pi R^2 \frac{n_0}{\tau_0}, \quad (1)$$

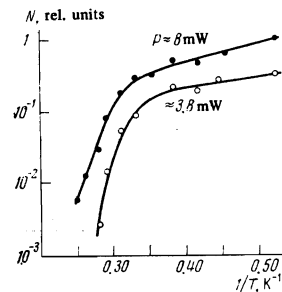


FIG. 9. Temperature dependence of EHD concentration at two different excitation intensities ($t_0 \lesssim 3 \mu \text{ sec}$).

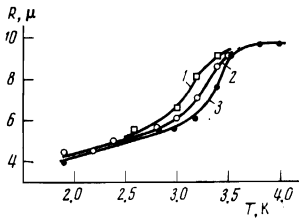


FIG. 10. Dependences of the EHD radius on the temperature at three different excitation intensities ($t_0 \leq 3 \mu\text{sec}$): 1) $P \approx 2.4 \text{ mW}$, 2) $P = 3.8 \text{ mW}$, 3) $P = 8 \text{ mW}$.

where n_0 and τ_0 are the equilibrium density and lifetime of the carriers in the condensed phase, and S is the flux of the excitons entering or leaving the drop:

$$S = 4\pi R^2 \gamma [n(R) - n_r(R)] v_T. \quad (2)$$

Here $n(R)$ is the concentration of the excitons near the surface of the drop, $v_T = (kT/2\pi M)^{1/2}$ is the thermal velocity of the excitons, M is their effective mass, γ is the "sticking coefficient" of the excitons in the drop, i. e., the probability that an exciton landing on the surface of the drop will be captured rather than reflected and

$$n_r(R) = v \left(\frac{M_d kT}{2\pi \hbar^2} \right)^{3/2} \exp \left(-\frac{\Delta}{kT} + \frac{2\alpha}{n_0 R kT} \right) \quad (3)$$

is the thermodynamic-equilibrium concentration of the excitons above a drop of radius R . In formula (3), Δ is the work function of the excitons from the EHD as $R \rightarrow \infty$, M_d is the effective mass of the density of state of the excitons, α is the coefficient of the surface tension of the electron-hole liquid, and ν is the multiplicity of the degeneracy of the ground state of the exciton (with respect to spin, the number of equivalent extrema in the Brillouin zone, etc.). The term $-4\pi R^2 \gamma n_r v_T$ in (2) describes the evaporation of the excitons from the drop, and the term $2\alpha/n_0 R kT$ in the argument of the exponential in (3) describes the increase of the evaporation rate due to the surface tension.

Equations of the type (1) and (3) were proposed by Pokrovskii and Svistunova in^[8] and used in a number of studies,^[7, 11, 13, 23, 25, 26] in all of which it was assumed, however, that the exciton concentration $n(R)$ near the surface of the drop coincides with their average concentration in the volume, and no account was taken of the role of the surface tension. Silver^[32] used a somewhat more general approach in the analysis of the structure of the two-phase system of the non-equilibrium carriers, based on equations of the Fokker-Planck type for the EHD radius distribution function, and demonstrated within the framework of this approach the need for taking the surface tension into account. However, the difference between $n(R)$ and n (averaged over the volume of the exciton concentration) was not taken into account in his paper. At the same time, the presence of an exciton-concentration drop is necessary for the existence of the flux S .

The dependence of the exciton concentration $n(\mathbf{r}, t)$

on the coordinate \mathbf{r} and on the time t is determined by the diffusion equation

$$\frac{\partial n(\mathbf{r}, t)}{\partial t} + \text{div}[-D\nabla n(\mathbf{r}, t)] + \frac{n(\mathbf{r}, t)}{\tau} = g(\mathbf{r}, t), \quad (4)$$

where D is the exciton diffusion coefficient, τ is their lifetime, and $g(\mathbf{r}, t)$ is the rate of generation of non-equilibrium carriers by the excitation source (it is assumed that the time of binding the carriers into excitons is short enough). Conditions (2) on the surface of each EHD serve as the boundary conditions for (4). Recognizing that the distance between the drops is much smaller than the exciton diffusion length $L_D = \sqrt{D\tau}$, we can average Eq. (4) over the volume elements containing many EHD but small relative to L_D . Then

$$\frac{\partial \bar{n}}{\partial t} + \text{div}(-D\nabla \bar{n}) + NS(\bar{n}, R) + \frac{\bar{n}}{\tau} = g(\mathbf{r}, t), \quad (5)$$

where $\bar{n}(\mathbf{r}, t)$ is the exciton concentration averaged in the indicated manner and N is the drop concentration. Equation (5) describes the time variation of the average exciton concentration $\bar{n}(\mathbf{r}, t)$ as the result of their generation, recombination, and diffusion, as well as capture and evaporation by the drops (the term $NS(\bar{n}, R)$). In the case of a spatially homogeneous excitation of the sample we have $\text{div}(-D\nabla \bar{n}) = 0$ and the diffusion fluxes of the excitons propagate only towards each of the drops.

To find $S(\bar{n}, R)$ it is necessary to solve (4) in the vicinity of each given drop with boundary conditions (2) and $n(r \rightarrow \infty) = \bar{n} \equiv n$ (it is assumed that the dimension of the drops is small in comparison with the distance between them). Since we are now dealing with the solution of the problem in a small region $r \ll N^{-1/3}$ (r is the distance from the center of the drop), within which a nonstationary exciton distribution is established in a rather short time, the terms with $\partial n/\partial t$, n/τ , and g can be omitted from (4), accurate to the small terms

$$NR^2 \ll 1, \quad (NL_D^3)^{-1} \ll 1. \quad (6)$$

Thus

$$D \text{div grad } n(r) = \frac{D}{r^2} \frac{d}{dr} \left(r^2 \frac{dn(r)}{dr} \right) = 0.$$

Inasmuch as $D\nabla n|_{r=R} = S/4\pi R^2$, the solution of this equation with allowance for the boundary conditions takes the form $n(r) = n - S/4\pi D r$. Combining it with (2) and (1) we obtain

$$S(n, R) = 4\pi \gamma R^2 \frac{n - n_r(R)}{1 + \gamma v_T R/D} v_T \quad (7)$$

and

$$\frac{dR}{dt} = \frac{n - n_r(R)}{n_0} \frac{\gamma v_T}{1 + \gamma v_T R/D} - \frac{R}{3\tau_0}. \quad (8)$$

For small drops, Eqs. (8), (5), and (3) differ from those usually employed^[7, 8, 11, 13, 23, 25, 26] only in that the surface tension is taken into account in the evaporation rate (3). However, when the dimensions of the drops

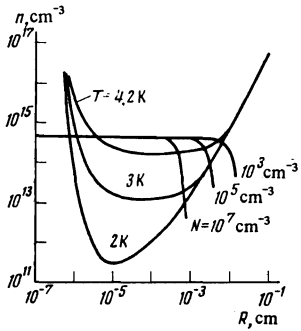


FIG. 11. Plots of n against R , calculated from formula (9) at three different temperatures and from formula (12) for three EHD concentrations at $\gamma=1$, $\tau_0=20 \mu\text{sec}$, $D=1500 \text{ cm}^2/\text{sec}$ at $T=3^\circ\text{K}$ ^[13] and with account taken of the fact that $D \sim T^{-1/2}$, $\tau=5 \mu\text{sec}$, and $g=10^{20} \text{ cm}^{-3}\text{sec}^{-1}$ (the numerical values of the remaining parameters are given in the text).

become comparable with the exciton mean free path ($v_T R/D \gtrsim 1$), their further growth is greatly slowed down by the strong decrease of the exciton concentration near the surfaces of the drops in comparison with their average concentration n in the volume.

In the stationary case, Eq. (8) determines directly the connection between the average exciton concentration and the EHD radius:

$$n = n_T(R) + \frac{n_0 R}{3\gamma v_T \tau_0} \left(1 + \gamma \frac{v_T R}{D} \right), \quad (9)$$

which is plotted in Fig. 11.

In the plane of the variables n and R (Fig. 11), the points that do not land on the $n=f(R)$ curve described by expression (9) cannot correspond to stationary states of the system. For points lying above this curve, the radius of the drop increases with time ($dR/dt > 0$), and for points lying below this curve it decreases ($dR/dt < 0$). Therefore the stable states are only those on the right-hand ascending branch of the $n=f(R)$ curve at $R > R_{\min}$, whereas on the descending (left) part any small deviations of n or R lead to the fact that R begins to vary with time, going farther and farther away from the equilibrium curve.^[32]

Thus, for each given temperature there exists a certain minimal radius defined by the relation

$$R_{\min}^2 \left(R_{\min} + \frac{D}{2\gamma v_T} \right) - \frac{3\alpha D \tau_0 n_T(R_{\min})}{n_0 k T} = 0, \quad (10)$$

so that in the stationary state the drops cannot have a dimension smaller than $R_{\min}(T)$. In the case $R \ll l \sim D/v_T$ is the exciton mean free path) we have

$$R_{\min} \approx \left(6\gamma \frac{\alpha v_T \tau_0 n_T}{n_0 k T} \right)^{1/2}, \quad (11)$$

where n_T is defined by (3). If furthermore $2\alpha/n_0 R k T \ll 1$, then this quantity can be neglected in the argument of the exponential in (3) and $n_T \approx n_{0T}$, i. e., it is nearly equal to the thermodynamic-equilibrium concentration of the excitons over the "liquid" in the case of a flat

interface.

The true value of R is determined by the EHD concentration by virtue of relations (5) and (9). If the excitation can be regarded as stationary and spatially-homogeneous with sufficient degree of accuracy, then with (7) and (8) taken into account, (5) can be transformed into (with allowance for the fact that $\partial n/\partial t = \partial R/\partial t = \text{div}(-D\nabla n) = 0$)

$$\frac{n}{\tau} + \frac{4}{3} \pi R^3 N \frac{n_0}{\tau_0} = g, \quad (12)$$

which reflects simply the balance of the number of generated and recombining carriers. Plots of the average concentration of the excitons n against the EHD radius, calculated with the aid of (12) for three different drop concentrations N , are also shown in Fig. 11. The points of intersection of these curves with the stable branch of the $n=f(R)$ curves described by expression (9) yield the radius of the EHD at a given drop concentration and at a given generation level, and the intersection with the unstable branch gives the "critical" radius of the nuclei.

It seems natural to assume that under conditions of stationary excitation, owing to the production of more and more new EHD, the value of N will increase with time, while n and R will decrease and tend gradually to their limiting values that are compatible with (9) and (12) and with the condition $R \geq R_{\min}$, namely

$$N_{\max}(g, T) = \frac{3}{4\pi} \frac{\tau_0}{n_0 R_{\min}^3} \left(g - \frac{n_{\min}(T)}{\tau} \right), \quad (13)$$

$$n_{\min}(T) = n(R_{\min}), \quad (14)$$

so that in this stationary state the EHD radius and concentration, as well as the density of the exciton gas, are determined by expressions (10), (13), and (14).

This is precisely the conclusion drawn by Silver.^[32] However, the data by others, which are cited above, do not agree with this conclusion. Indeed, as seen from Figs. 3, 8, and 10, at the same temperature $T \lesssim 3^\circ\text{K}$, the EHD radii vary noticeably as functions of the excitation level and the rise time of the exciting pulse, in contrast to R_{\min} , which depends only on T . At $T \gtrsim 3.5^\circ\text{K}$, the radii in general are practically independent of T ($R \approx 10 \mu$), whereas R_{\min} should increase monotonically with temperature. Finally, numerical values of the observed EHD radii also exceed noticeably the values of R_{\min} estimated from formula (11), especially at low temperatures ($T \approx 2^\circ\text{K}$). Assuming $\gamma \approx 1$, $\alpha \sim 2 \times 10^{-4} \text{ erg/cm}^2$,^[16,31] $M = M_d \approx 4 \times 10^{-28} \text{ g}$, $\tau = 40 \mu\text{sec}$, $n_0 \approx 2 \times 10^{17} \text{ cm}^{-3}$, $\nu = 16$, and $\Delta \approx 2.1 \text{ meV}$ we obtain the values $R_{\min} \approx 5 \mu$ and $\approx 0.2 \mu$ at $T = 4.2^\circ\text{K}$ and 2°K , respectively. Thus, if the observed values of R can be close to R_{\min} then this can occur only at the highest temperatures near 4°K . There is no doubt, however, that the condition $R > R_{\min}$ is satisfied by all the experimental values of R .

All these facts indicate that under the conditions of our experiments, in spite of the long duration of the exciting pulses, greatly exceeding the lifetimes of both

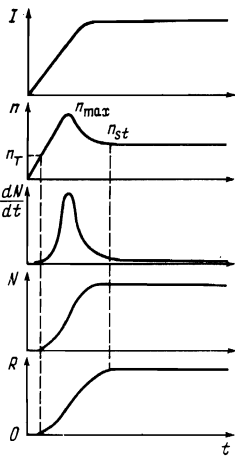


FIG. 12. Plots of the exciton concentration n , of the EHD N , of the rate of nucleus formation dN/dt , and of the drop radius R on the time t with increasing excitation intensity I in the pulse.

the excitons and the EHD, the system is still far from the stationary state described by formulas (13) and (14). This is indicated primarily by the strong dependence of the EHD number on the duration of the front of the exciting pulse. Indeed, the front duration during which the excitation varies with time, is not more than 20% of the pulse duration during which the excitation is perfectly stationary, and the EHD concentration in the case of a short rise time of the exciting pulse nevertheless greatly exceeds the value observed in the case of a slow growth of the excitation. This seems to mean that the EHD or their nuclei are produced only at the very start of the pulse and that their number then remains practically constant during the entire remainder of the pulse. This result can be explained qualitatively in the following manner:

When the exciting pulse is applied, the exciton concentration n in the sample begins to increase (Fig. 12). When this concentration greatly exceeds n_{0T} , EHD nuclei begin to form, but the number of excitons going to these nuclei is relatively small at first, since both the number of the nuclei N and the radius of each of the nuclei are small, so that the term $NS \sim NR^2$ plays no role in (5). Therefore the exciton concentration continues to increase (within times shorter than τ or, in the case of a long rise time—shorter than the front duration). But with increasing degree of supersaturation of the electron gas, the number of the newly produced nuclei increases rapidly (exponentially), and the radii of the previously produced EHD increase with them, in accord with (8). At a certain instant, the number of excitons going into the drops becomes comparable with the rate of carrier generation, and later it even exceeds it. From this instant on, the exciton concentration begins to decrease, in spite of the constant or even increasing excitation intensity I , since all the produced excitons are required for the growth and for the maintenance of the existence of the already produced EHD. The formation of new nuclei, on the other hand, soon practically ceases, because the exciton concentration decreases to a level to n_{st} , at which the probability of production of nuclei, meaning also the rate of their formation dN/dt , is very small. The previously produced EHD continue to increase for some time, until they reach the dimension determined

by formulas (9) and (12), but now already at a given number of EHD.²⁾

At first glance, the following considerations, based on the stabilization of the concentration of the excitons at a level close to n_{0T} contradict certain known results,^[13,17] which show that even under stationary excitation, especially at temperatures $T > 3^\circ\text{K}$, the number of excitons continues to increase with increasing excitation level after passing through the condensation threshold. This, however, is more readily due to the fact that in all the experiments, as was already emphasized in^[32], the excitation is not spatially homogeneous and the condensation threshold is reached first in a very narrow region, where the excitation is maximal. With further rise of the carrier generation level, the number of excitons continues to grow on account of those regions where the condensation threshold has not yet been reached. The increase in the dimensions of the region in which the EHD are concentrated with increasing excitation was noted by many workers.^[38-42] It is seen also in our experiments on Fig. 5. At the same time, the above-described time evolution of the exciton condensation process agrees not only with our data, but also with the well-known results^[17,18] on the observation of hysteresis phenomena in the EHD and exciton radiation, results which can hardly be explained in any other way.

A more detailed examination of this evolution (Appendix) on the basis of the well-known theory of formation of critical nuclei of a liquid phase in supersaturated vapor^[43-45] explains practically all the qualitative features of our experimental results.

Indeed, formulas (A.35) and (A.37) show that the drop concentration N increases with decreasing rise time t_0 of the exciting pulse, in agreement with the results shown in Figs. 4, 6, and 9. With decreasing temperature, N first increases very rapidly, and this growth is stronger in the case of a short rise time (A.37) than a long one (A.35). The experimentally observed slopes of $\log N$ against $1/T$ (Fig. 4) are well represented by these formulas at $\Delta \approx 20-25^\circ\text{K}$, which agrees with the *spectroscopically* determined work function of the excitons from the EHD, $\Delta \approx 2$ meV. With further decrease of temperature, the growth of N decreases very rapidly ($\beta\xi$ in (A.35) and $\beta\eta$ in (A.37) become of the order of unity), as is clearly seen from Figs. 6 and 9. The dependence of N on the excitation level g is, in accordance with (A.37), stronger (super-linear) for a short front than for a long one—see (A.35). It becomes steeper with increasing temperature; for example, in the case of a short front, as T approaches the condensation threshold at a given g , the delay time t_m of the drop formation increases, and when it becomes larger than t_0 we go over from the short-front situation described by formula (A.37) to the case of “extremely short front,” described by formula (A.21); we change from the relation $N \propto g^{3/2}$ to $N \propto g^3$. All these results agree qualitatively with those shown in Fig. 7.

We have not carried out a detailed quantitative re-

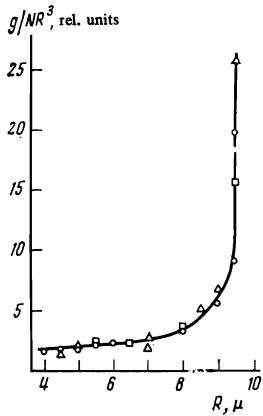


FIG. 13. Plot of g/NR^3 against R at three different excitation levels: $\circ - P \approx 8$ mW, $\Delta - P \approx 3.8$ mW, $\square - P \approx 2.4$ mW.

duction of the experimental results by means of the theoretical formulas, inasmuch as these results are known to be distorted by the aforementioned expansion of the spatial region of concentration with decreasing temperature or with rising excitation level. We note, however, that formulas (A.35) and (A.37) yield the correct order of magnitude of not only the qualitative relations but also of the absolute values of the EHD concentrations. Thus, for example, for the case $t_0 = 3$ μ sec, assuming $\Delta \approx 2.1$ mV, $\alpha \approx 2 \times 10^{-4}$ erg/cm², $g\tau \approx 5 \times 10^{13}$ cm⁻³ (which corresponds to an excitation power ≈ 8 mW under the conditions of our experiment), $\tau = 5$ μ sec, and $N_i \approx 10^{12}$ cm⁻³ and taking the values of these parameters given above for Ge, we obtain from (A.37) and (A.38) the values $N \sim 4 \times 10^5$ and $\sim 10^7$ cm⁻³ at $T = 3.2$ and 2.8 $^\circ$ K, respectively, in reasonable agreement with the result shown in Fig. 4. We note also that these calculated values depend very little on the choice of the number N_i of the condensation centers.

In conclusion, let us discuss the behavior of the EHD radius. Figure 13 shows the dependence of the ratio of the generation rate to the volume of the liquid phase, g/NR^3 , on the EHD radius for three different generation levels. At small R (low temperatures), $g/NR^3 \approx$ constant, as follows from (12) in the case when the recombination in the gas phase can be neglected. At large EHD radii (high temperatures), however, the radius exhibits a clearly pronounced tendency to the value ≈ 10 μ (Figs. 3, 8, 10), which depends neither on the temperature nor on the level and the method of excitation. This tendency is particularly clearly manifest in Fig. 13 by the abrupt growth of g/NR^3 at a practically constant value of the radius. This result cannot be described by expressions (9) and (12), which seems to indicate that the theoretical picture described above is incomplete.

The experimental data indicate that there exists a certain mechanism that limits strongly the growth of the EHD radius at $R \sim 10$ μ , at least under the conditions of our experiments. At the present time we are unable to explain this fact finely. A number of possible mechanisms that limit the EHD radius have been considered in^[46, 47].

We are indebted to S. G. Tikhodeev for a discussion of the results.

APPENDIX

The well-known formula^[45] for the rate of production of critical nuclei in supersaturated vapor with particle density n can be represented in the form

$$\frac{dN}{dt} = A \left(\frac{\beta \Delta}{kT} \right)^{1/2} v_r n_0^{1/2} N_i \frac{n}{n_0} \exp \left\{ -\lambda(T) / \ln^2 \frac{n}{n_0} \right\}, \quad (\text{A.1})$$

where

$$\lambda(T) = \frac{2\pi}{3} \left(\frac{2\beta \Delta}{kT} \right)^3. \quad (\text{A.2})$$

The dimensionless coefficient β is connected with the surface-tension coefficient α by the relation

$$\alpha = \beta \Delta n_0^{1/2}, \quad (\text{A.3})$$

N_i is the concentration of the impurities that serve as condensation centers, $n_{0T} = n_T(R = \infty)$ is the equilibrium density of the saturated vapor over the planar phase-separation boundary, and A is a numerical factor of the order of unity. Strictly speaking, the numerical factor in the pre-exponential term of (A.1) can be omitted, since inclusion of this factor is an exaggeration of the accuracy with which this formula is derived. We shall therefore omit from all the final formulas the numerical pre-exponential factors.

Equations (5), (7), (8), and (A.1) form a complete system of equations describing exciton condensation. We consider the case of a long (with duration much larger than τ) pulse of spatially homogeneous excitation $g(t)$, beginning with the instant $t = 0$ ($g(t < 0) = 0$). At the start of the pulse, in the absence of EHD, the exciton concentration increases monotonically in accordance with the regular law

$$n(t) = \int_0^t \exp \left\{ -\frac{t-t'}{\tau} \right\} g(t') dt'. \quad (\text{A.4})$$

Formation of the EHD begins at the instant of time t_1 at which $n(t_1)$ reaches the value n_{0T} , and their contribution to the change in the number of free excitons can be represented in the form

$$-N(t)S(n, R) = -4\pi v_r \int_{t_1}^t \frac{dN(t')}{dt'} \frac{R^2(t, t')}{1 + v_r R(t, t')/D} [n - n_r(R(t, t'))] dt', \quad (\text{A.5})$$

where $R(t, t')$ is the value, at the instant t , of the radius of the drop produced at the instant t' , i. e., the solution of equation (8) with initial condition $R(t') = 0$. With (A.5) taken into account, Eq. (5) takes the form

$$\frac{\partial n}{\partial t} = g(t) - \frac{n}{\tau} - 4\pi v_r \int_{t_1}^t \frac{dN(t')}{dt'} \frac{R^2(t, t')}{1 + v_r R(t, t')/D} [n(t) - n_r(R(t, t'))] dt'. \quad (\text{A.6})$$

Recognizing that $\lambda \gg 1$, we can easily see that so long as the supersaturation of the exciton gas is small, $(n - n_{0T})/n_{0T} \ll 1$, the contribution of the last term in the right-hand side of (A.6) is negligibly small, but with increase of supersaturation, at $(n - n_{0T})/n_{0T} \gtrsim 1$, it begins to grow very rapidly, and at a certain instant

t_m the right-hand side of (A.6) reverses sign, i.e., the exciton concentration reaches the maximum value n_m , which is connected with t_m by the relation

$$g(t_m) - \frac{n_m}{\tau} - 4\pi v_T \int_{t_i}^{t_m} \frac{dN(t')}{dt'} \frac{R^2(t_m, t')}{1 + v_T R(t_m, t')/D} [n_m - n_T(R(t_m, t'))] dt' = 0. \quad (\text{A.7})$$

By virtue of the very strong dependence of dN/dt on n , the main contribution to the integral in (A.7), as well as in all the subsequently encountered integrals containing dN/dt , is made by a narrow vicinity of the instant of time t_m . Therefore, expanding the argument of the exponential in (A.1) in terms of the small difference $t_m - t' = s \ll t_m$, we obtain

$$\frac{dN}{dt'} \approx A \left(\frac{\beta \Delta}{kT} \right)^{1/2} v_T n_0^{1/2} N_i \frac{n_m}{n_0} \exp \left\{ -\frac{\lambda}{\mathcal{L}^2} + \frac{\lambda}{n_m \mathcal{L}^2} n_m'' s^2 \right\}, \quad (\text{A.8})$$

where $\ln(n_m/n_{0T}) \equiv \mathcal{L}$, $n_m'' = (\partial^2 n / \partial t^2)_{t=t_m}$ appeared. To find n_m'' we differentiate (A.6) once more with respect to time at the instant $t = t_m$, recognizing that $(\partial n / \partial t)_{t_m} = 0$ and $R(t_m, t_m) = 0$:

$$n_m'' = \left(\frac{dg}{dt} \right)_{t_m} - 4\pi v_T \int_{t_i}^{t_m} \frac{dN(t')}{dt'} \frac{d}{dt_m} \times \left\{ \frac{R^2(t_m, t')}{1 + v_T R(t_m, t')/D} [n_m - n_T(R(t_m, t'))] \right\} dt'. \quad (\text{A.9})$$

Using (A.8), we usually obtain the total number of the produced EHD:

$$N \approx \int_{-\infty}^{\infty} \frac{dN(t_m - s)}{ds} ds \approx A \pi^{1/2} \left(\frac{\beta \Delta}{kT} \right)^{1/2} \left(\frac{n_m \mathcal{L}^3}{\lambda |n_m''|} \right)^{1/2} v_T n_0^{1/2} N_i \frac{n_m}{n_0} \exp \left\{ -\frac{\lambda}{\mathcal{L}^2} \right\} = \frac{\sqrt{3}}{4} \frac{kT}{\beta \Delta} \frac{v_T N_i}{n_0^{3/2}} \left(\frac{n_m \mathcal{L}^3}{|n_m''|} \right)^{1/2} \exp \left\{ -\frac{\lambda}{\mathcal{L}^2} \right\}. \quad (\text{A.10})$$

On the other hand, the calculation of the analogous integrals in (A.7) and (A.9) calls for an additional analysis of the properties of the integrands. The point is that as $t' \rightarrow t_m$ the radius R tends to zero, or more accurately to the radius of the critical nucleus

$$R_c(n) = \frac{2\beta \Delta}{kT \ln(n/n_{0T})} n_0^{-1/2}. \quad (\text{A.11})$$

The difference $n - n_T(R)$ tends to zero at the same time. We cannot therefore replace in (A.7) and (A.9) all the factors by their values at $s = 0$, with the exception of dN/dt . However, with increasing s , the radius $R(t_m, t_m - s)$ increases in accordance with (8) like

$$\frac{n}{n_0} v_T s = \int_{(1+\delta)R_c}^{R(t_m, t_m - s)} dR \left(1 - \exp \left\{ -\frac{R - R_c}{R} \ln \frac{n}{n_{0T}} \right\} \right)^{-1}, \quad (\text{A.12})$$

where $\delta \cdot R_c$ is the initial excess of the radius above the critical value at $t' = t_m - s$ ($0 < \delta \leq 1$).

In the derivation of (A.12) we took into account the fact that we are dealing here with very small time intervals and radii, so that the terms in (8), which describe the recombination and diffusion, were left out.

In addition, it was assumed that $\gamma = 1$ and that the exciton concentration n at the instant $t' = t_m - s$ does not change significantly in the interval s . It is easy to verify that if the condition

$$\frac{n}{n_0} \frac{v_T s}{R_c} \gg \frac{1}{\ln(n/n_{0T})} \quad (\text{A.13})$$

is satisfied, the EHD radius begins to depend linearly on s , and the difference become $n - n_T(R) \approx n - n_{0T}$. We shall see later on that for values of s that make the effective contribution to the integrals of (A.7) and (A.9), the condition (A.13) is satisfied practically in all cases when the condensation is observable. Then, taking all the foregoing into account we have

$$R^2(t_m, t_m - s) [n_m - n_T(R(t_m, t_m - s))] \approx \frac{(n_m - n_{0T})^2}{n_0^2} v_T^2 s^2; \\ g(t_m) - \frac{n_m}{\tau} - \pi^{1/2} A \left(\frac{\beta \Delta}{kT} \right)^{1/2} v_T^2 N_i n_0^{1/2} n_m \left(\frac{n_m - n_{0T}}{n_0} \right)^2 \times \left(\frac{n_m \mathcal{L}^3}{\lambda |n_m''|} \right)^{1/2} \exp \left\{ -\frac{\lambda}{\mathcal{L}^2} \right\} = 0 \quad (\text{A.14})$$

and

$$n_m'' = \left(\frac{dg}{dt} \right)_{t_m} - 4\pi A \left(\frac{\beta \Delta}{kT} \right)^{1/2} v_T^2 N_i n_0^{1/2} \left(\frac{n_m - n_{0T}}{n_0} \right)^2 \frac{n_m \mathcal{L}^3}{\lambda |n_m''|} \exp \left\{ -\frac{\lambda}{\mathcal{L}^2} \right\}. \quad (\text{A.15})$$

Recognizing that the effective values of $s \ll t_m$ and $g(t)$ vary with time much more slowly than the last term in (A.6), we can determine the instant of time t_m by using directly Eq. (A.4) in the form

$$n_m \approx \int_0^{t_m} g(t) \exp \left\{ -\frac{t_m - t}{\tau} \right\} dt. \quad (\text{A.16})$$

Formula (A.10) together with equations (A.14)–(A.16) solves completely in principle the problem of the number of produced EHD for sufficiently long pulses (large t_m) of volume excitation. However, the character of the resultant dependences of N on g and T can be quite different under different experimental conditions. We demonstrate this by considering certain limiting cases, assuming that the excitation intensity first increases linearly with time, and then levels off at the stationary value

$$g(t) = \begin{cases} gt/t_0, & 0 \leq t \leq t_0 \\ g, & t > t_0 \end{cases}. \quad (\text{A.17})$$

1. Extremely short rise time of the exciting pulse: $t_0 \rightarrow 0$. The EHD production occurs at $t > t_0$, i.e., $(dg/dt)_{t_m} = 0$. In this case

$$N = \text{const} \left[\left(\frac{kT}{\beta \Delta} \right)^{1/2} \frac{N_i}{n_m - n_{0T}} \mathcal{L} \right]^{1/2} n_m \exp \left\{ -\frac{3}{4} \frac{\lambda}{\mathcal{L}^2} \right\}, \quad (\text{A.18})$$

and n_m is determined by the transcendental equation

$$g - \frac{n_m}{\tau} = \left(\frac{\pi^3 A}{8} \right)^{1/2} \left[\left(\frac{\beta \Delta}{kT} \right)^{1/2} N_i n_0^{1/2} \right]^{1/2} n_m v_T \left(\frac{n_m - n_{0T}}{\lambda n_0} \right)^{1/2} \mathcal{L}^{1/2} \exp \left\{ -\frac{1}{4} \frac{\lambda}{\mathcal{L}^2} \right\}. \quad (\text{A.19})$$

In (A.18) and the sequel, the constant stands for a numerical factor on the order of unity. At low excesses

of the excitation level above threshold, $g_T = n_{0T}/\tau$, so long as

$$\left(\frac{\beta\Delta}{kT}\right)^{1/2} N_i n_0^{1/2} (v_T\tau)^{1/2} \left[\frac{kT}{\beta\Delta} \ln \frac{g\tau}{n_{0T}}\right]^3 \left(\frac{g\tau - n_{0T}}{n_0}\right)^3 \exp\left\{-\frac{\lambda}{\ln^2(g\tau/n_{0T})}\right\} \ll 1, \quad (\text{A.20})$$

we have $t_m \gg \tau$ and $n_m \approx g\tau$, so that the number of the produced EHD is given by formula (A.18), in which n_m is replaced everywhere by $g\tau$.

At a higher excitation level or at lower temperatures, when an inequality inverse to (A.20) is satisfied, t_m becomes smaller than τ , and $n_m \ll g\tau$, while formulas (A.18) and (A.19) can be reduced to

$$N = \text{const} \cdot \left(\frac{g}{N_T v_T}\right)^3 \left(\frac{n_0}{N_T}\right)^2 \frac{1}{\xi^6} \exp\left\{5 \frac{\Delta}{kT} [1 - (0.762\pi)^{1/2} \beta \xi]\right\}, \quad (\text{A.21})$$

where

$$N_T = v(M_e kT / 2\pi \hbar^2)^{3/2}, \quad (\text{A.22})$$

and the dimensionless parameter ξ is defined by the relation

$$\xi = \left(\frac{7}{\lambda}\right)^{1/2} \mathcal{L} = \left(\frac{21}{16\pi}\right)^{1/2} \frac{kT}{\beta\Delta} \mathcal{L} \quad (\text{A.23})$$

and is determined from the equation

$$\frac{1}{\xi^2} - \xi - \frac{9}{7} \left(\frac{21}{16\pi}\right)^{1/2} \frac{kT}{\beta\Delta} \ln \xi = \left(\frac{21}{16\pi}\right)^{1/2} \frac{kT}{7\beta\Delta} \ln \left[\left(\frac{\beta\Delta}{kT}\right)^{1/2} N_i n_0^{1/2} \left(\frac{n_{0T}}{g}\right)^3 \left(\frac{n_{0T} v_T}{g}\right)^2\right], \quad (\text{A.24})$$

which follows directly from (A.19) and (A.23) at $t_m \ll \tau$.

2. Production of EHD on the front of the exciting pulse ($t_m < t_0$). In this case it follows from (A.16) and (A.17) that $(dg/dt)_{t_m} = g/t_0$ and

$$n_m = \frac{g\tau^2}{t_0} \left(\frac{t_m}{\tau} - 1 + e^{-t_m/\tau}\right). \quad (\text{A.25})$$

After determining n_m'' from (A.15) and introducing, to simplify the subsequent formulas, the notation

$$\chi = 1 - e^{-t_m/\tau}, \quad (\text{A.26})$$

$$G = g\tau^2/n_{0T} t_0, \quad (\text{A.27})$$

$$\Lambda = 64A \left(\frac{\beta\Delta}{kT}\right)^{1/2} N_i n_0^{1/2} (v_T\tau)^{1/2}, \quad (\text{A.28})$$

we reduce equations (A.14) and (A.25) to the form

$$\chi = \frac{1}{8} \left[\frac{2\pi}{\lambda G} \frac{n_m}{n_{0T}} \mathcal{L}^3\right]^{1/2} \frac{F(n_m, G)}{\{[1+F(n_m, G)]^{1/2} - 1\}^{3/2}}, \quad (\text{A.29})$$

$$G^{-1} \frac{n_m}{n_{0T}} = -[\chi + \ln(1-\chi)], \quad (\text{A.30})$$

where

$$F(n_m, G) = \frac{\pi}{4\lambda} \frac{\Lambda}{G^2} \left(\frac{n_m}{n_{0T}}\right)^2 \left(\frac{n_m - n_{0T}}{n_0}\right)^3 \mathcal{L}^3 \exp\left(-\frac{\lambda}{\mathcal{L}^2}\right). \quad (\text{A.31})$$

Obviously, by virtue of the definition of χ , the condition $t_m < t_0$ corresponds to $\chi < 1 - e^{-t_0/\tau}$. This condition can be satisfied, naturally, only after a certain minimum excitation level G_{\min} is reached, defined by

the relation

$$1 - e^{-t_0/\tau} = \frac{1}{8} \left[\frac{2\pi}{\lambda G_{\min}} \frac{n(G_{\min}, t_0)}{n_{0T}} \ln^2 \frac{n(G_{\min}, t_0)}{n_{0T}}\right]^{1/2} \times \frac{F(n(G_{\min}, t_0), G_{\min})}{\{[1+F(n(G_{\min}, t_0), G_{\min})]^{1/2} - 1\}^{3/2}}$$

in which $n(G_{\min}, t_0)$ is given by formula (A.25) with $G = G_{\min}$ and $t_m = t_0$. At $G < G_{\min}$ we have $t_m > t_0$ and the process of EHD production, in spite of the finite rise time of the exciting pulse, is described by the formulas considered above for the case $t_0 \rightarrow 0$. At excitation levels noticeably exceeding G_{\min} , we have $t_m < t_0$ and it is easy to show that the inequality $F(n_m, G) \ll 1$, is satisfied, and when this inequality is taken into account (A.10) and equations (A.29) and (A.30) can be reduced to the form:

$$N = \text{const} \cdot \left[\left(\frac{\beta\Delta}{kT}\right)^{1/2} \frac{N_i n_m}{n_{0T}^2} G\right]^{1/2} \frac{n_0^{3/2}}{v_T\tau} \left(\frac{n_m}{n_{0T}} - 1\right)^{-3/2} \exp\left\{-\frac{\lambda}{2\mathcal{L}^2}\right\} \quad (\text{A.32})$$

$$G^{-1} \frac{n_m}{n_{0T}} + \left[\frac{G n_{0T}}{\Lambda n_m} \left(\frac{n_0}{n_m - n_{0T}}\right)^3\right]^{1/2} \exp\left\{\frac{\lambda}{2\mathcal{L}^2}\right\} = -\ln \left\{1 - \left[\frac{G n_{0T}}{\Lambda n_m} \left(\frac{n_0}{n_m - n_{0T}}\right)^3\right]^{1/2} \exp\left\{\frac{\lambda}{2\mathcal{L}^2}\right\}\right\}. \quad (\text{A.33})$$

As written, formulas (A.32) and (A.33) are still not clear enough. They can however, be, noticeably simplified in two limiting cases, which we shall somewhat arbitrarily call the case of the short ($t_m \ll \tau$) and long ($t_m \gg \tau$) rise times of the exciting pulse. These cases are realized at $G \gg G_c$ and $G \ll G_c$, respectively, where G_c is determined by the equality

$$\frac{\lambda}{\ln^2 G_c} - 3 \ln(G_c - 1) = \ln \left[\Lambda \left(\frac{n_{0T}}{n_0}\right)^3\right]. \quad (\text{A.34})$$

It is obvious that the case of a long front is not realized at all at t_0 and the case of a short front can be realized also at $t_0 \lesssim \tau$, provided that the excitation level is high enough.

a) Case of long front ($G_{\min} < G < G_c$). In this case

$$N = \text{const} \cdot \frac{g n_0^2}{N_T^2 v_T^2 \tau t_0} \exp\left\{\frac{3\Delta}{kT} \left[1 - 2\left(\frac{\pi}{6}\right)^{1/2} \beta \xi\right]\right\}, \quad (\text{A.35})$$

where $\xi \equiv (4/\lambda)^{1/3} \mathcal{L}$ is defined by the equation

$$\frac{1}{\xi^2} - \xi = \frac{1}{8} \left(\frac{6}{\pi}\right)^{1/2} \frac{kT}{\beta\Delta} \ln \left[\frac{\Lambda}{G} \left(\frac{n_{0T}}{n_0}\right)^3\right]. \quad (\text{A.36})$$

Formula (A.35) is accurate to within a factor $(1 - n_{0T}/n_m)^3$ close to unity. At relatively high temperatures and at not too high excitation level, when $(\Lambda/G)(n_{0T}/n_0)^3 \gg 1$, we have $\beta\xi \ll 1$ and N increases quite rapidly with decreasing temperature. At low temperatures, however, this growth slows down.

b) Case of short front ($G > G_c$). In this case

$$N = \text{const} \cdot \left(\frac{g}{N_T v_T^2 t_0}\right)^2 \left(\frac{n_0}{N_T}\right)^2 \exp\left\{\frac{7}{2} \frac{\Delta}{kT} \left[1 - 2\left(\frac{2\pi}{15}\right)^{1/2} \beta \eta\right]\right\} \quad (\text{A.37})$$

The parameter $\eta \equiv (5/\lambda)^{1/3} \mathcal{L}$ is defined by the equation

$$\frac{1}{\eta^2} - \eta = \frac{1}{10} \left(\frac{15}{2\pi} \right)^{1/2} \frac{kT}{\beta\Delta} \ln \left[\frac{2\Lambda}{G^2} \left(\frac{n_{0T}}{n_0} \right)^3 \right]. \quad (\text{A. 38})$$

We discuss now the reason of applicability of the approximation used above. The entire analysis was based on the assumption that the time interval

$$s_{\text{eff}} = (n_m \mathcal{L}^3 / \lambda |n_m''|)^{1/2} \quad (\text{A. 39})$$

is short enough

$$s_{\text{eff}} \ll t_m, \quad (\text{A. 40})$$

but is at the same time long enough for the drops to grow to dimensions $R \gg R_c$ (the condition (A.13)).

We consider first the case of an extremely short front. Using (A.15), (A.16), (A.19), and (A.39) we easily obtain the ratio

$$\frac{s_{\text{eff}}}{t_m} = \frac{\tau}{t_m} (e^{t_m/\tau} - 1) \left(\frac{1}{\lambda} \mathcal{L}^3 \right)^{1/2}, \quad (\text{A. 41})$$

which shows that (A.40) is practically always satisfied by virtue of $\mathcal{L}^3 \ll \lambda$.

In the case of a front of finite duration we obtain from (A.15), (A.26), (A.39), and (A.29), assuming again $F \ll 1$, the estimate

$$s_{\text{eff}} \sim \tau (1 - e^{-t_m/\tau}),$$

from which it follows that the condition $s_{\text{eff}} \ll t_m$ is satisfied for a long front, and for a short front it is at the limit, i. e., $s_{\text{eff}} \sim t_m$. Thus, in this last case formulas (A.37) and (A.38) can claim only to describe the qualitative relations and the orders of magnitude.

The (second criterion (A.13) reduces in the cases of long, short, and extremely short fronts, to the respective forms

$$\frac{n_0 \lambda^{1/2}}{n_m \mathcal{L}^2} \ll n_0^{1/2} v_T \tau, \quad (\text{A. 42})$$

$$\left(\frac{g\tau^2}{n_m t_0} \right)^{1/2} \frac{n_0 \lambda^{1/2}}{n_m \mathcal{L}^2} \ll n_0^{1/2} v_T \tau, \quad (\text{A. 43})$$

$$\frac{g\tau n_0 \lambda^{1/2}}{n_m^2 \mathcal{L}^3} \ll n_0^{1/2} v_T \tau. \quad (\text{A. 44})$$

Satisfaction of these conditions does not follow automatically from any of the assumptions made above. However, in view of the fact that their right-hand sides contain the very large quantity $n_0^{1/2} v_T \tau \sim 10^7$ (for germanium), it is practically always satisfied when condensation is observable, i. e., at $n_m \gtrsim 10^{11} - 10^{12} \text{ cm}^{-3}$.

¹A value $\alpha \approx 1.6 \times 10^{-4} \text{ erg/cm}^2$ is cited in^[16,31]. However, formula (2) of^[31] is incorrect. To obtain the correct formula it is necessary to replace $\ln(T_0/T)$ in (2) by the quantity $[(T_0 - T)/T_0 + 3/2(kT/\varepsilon_0) \ln(T_0/T)]$. The reduction of the experimental result obtained in^[31] by means of the corrected formulas does not change the qualitative conclusions of the paper, and the corrected value of the surface-tension coefficient is $\alpha = 1.8 \times 10^{-4} \text{ erg/cm}^2$. We are grateful to D. Hensel for calling our attention to this circumstance.

²Similar arguments were advanced in^[37].

- ¹L. V. Keldysh, Proc. Trudy, Ninth Intern. Conf. on Physics of Semiconductors, Moscow, 1968, vol., Nauka, Leningrad (1969), p. 1387.
- ²V. M. Asinin and A. A. Pogachev, Pis'ma Zh. Eksp. Teor. Fiz. **9**, 415 (1969) [JETP Lett. **9**, 248 (1969)].
- ³Ya. E. Pokrovskii and K. I. Svistunova, *ibid.*, 435 [261].
- ⁴V. S. Vavilov, V. A. Zayats, and V. N. Murzin, *ibid.* **10**, 304 (1969) [10, 192 (1969)].
- ⁵B. S. Bagaev, T. I. Galkina, O. V. Gogolin, and L. V. Keldysh, *ibid.*, 309 [195].
- ⁶L. V. Keldysh, Usp. Fiz. Nauk **100**, 514 (1970) [Sov. Phys. Usp. **13**, 292 (1970)].
- ⁷L. V. Keldysh, in: Eksitony v poluprovodnikakh (Excitons in Semiconductors), Nauka, 1971, p. 5.
- ⁸Ya. E. Pokrovskii and K. I. Svistunova, Fiz. Tekh. Poluprovodn. **4**, 491 (1970) [Sov. Phys. Semicond. **4**, 409 (1970)].
- ⁹A. S. Alekseev, V. S. Bagaev, T. I. Galkina, O. V. Gogolin, and N. A. Penin, Fiz. Tverd. Tela **12**, 3516 (1970) [Sov. Phys. Solid State **12**, 2855 (1971)].
- ¹⁰V. S. Bagaev, T. I. Galkina, and O. V. Gogolin, Proc. Tenth Intern. Conf. on Physics of Semiconductors, Cambridge, Mass., 1970, publ. by US Atomic Energy Commission, Washington, DC (1970), p. 500.
- ¹¹Ya. Pokrovsky, A. Kaminsky, K. Svistunova, *ibid.*, p. 504.
- ¹²V. S. Vavilov, V. A. Zayats, and V. N. Murzin, *ibid.*, p. 509.
- ¹³Ya. E. Pokrovskii, Phys. Status Solidi [a] **11**, 385 (1972).
- ¹⁴B. V. Zubov, V. P. Kalinushkin, T. M. Murina, A. M. Prokhorov, and A. A. Pogachev, Fiz. Tekh. Poluprovodn. **7**, 1614 (1973) [Sov. Phys. Semicond. **7**, 1077 (1974)].
- ¹⁵V. S. Bagaev, N. A. Penin, N. N. Sibel'din, and V. A. Tsvetkov, Fiz. Tverd. Tela **15**, 3269 (1973) [Sov. Phys. Solid State **15**, 2179 (1974)].
- ¹⁶A. S. Alekseev, T. A. Astemirov, V. S. Bagaev, T. I. Galkina, N. A. Penin, N. N. Sybeldin, and V. A. Tsvetkov, Proc. Twelfth Intern. Conf. on Physics of Semiconductors, Stuttgart, 1974, p. 91.
- ¹⁷T. K. Lo, B. J. Feldman, and C. D. Jeffries, Phys. Rev. Lett. **31**, 224 (1973).
- ¹⁸T. K. Lo, B. J. Feldman, R. M. Westervelt, J. L. Staehli, C. D. Jeffries, and E. E. Haller, Preprint, 1975.
- ¹⁹V. S. Bagaev, T. I. Galkina, and O. V. Gogolin, in: Eksitony v poluprovodnikakh (Excitons in Semiconductors), Nauka, 1971, p. 19.
- ²⁰C. Benoit a la Guillaume and M. Voos, Phys. Rev. [B] **7**, 1723 (1973).
- ²¹G. A. Thomas, T. G. Phillips, T. M. Rice, and J. C. Hensel, Phys. Rev. Lett. **31**, 386 (1973).
- ²²T. K. Lo, Solid State Commun. **15**, 1231 (1974).
- ²³J. C. Hensel, T. G. Phillips, and T. M. Rice, Phys. Rev. Lett. **30**, 227 (1973).
- ²⁴J. C. McGroddy, M. Voos, and O. Christensen, Solid State Commun. **13**, 1801 (1973).
- ²⁵C. Benoit a la Guillaume, M. Capizzi, B. Etienne, and M. Voos, Solid State Commun. **15**, 1031 (1974).
- ²⁶R. M. Westervelt, T. K. Lo, J. L. Staehli, and C. D. Jeffries, Phys. Rev. Lett. **32**, 1051 (1974).
- ²⁷T. M. Rice, Phys. Rev. [B] **9**, 1540 (1974).
- ²⁸L. M. Sander, H. B. Shore, and L. J. Sham, Phys. Rev. Lett. **31**, 533 (1973).
- ²⁹H. Büttner and E. Gerlach, J. Phys. C **6**, L 433 (1973).
- ³⁰T. L. Reinecke and S. C. Ying, Solid State Commun. **14**, 381 (1974).
- ³¹V. S. Bagaev, N. N. Sibel'din and V. A. Tsvetkov, Pis'ma Zh. Eksp. Teor. Fiz. **21**, 180 (1975) [JETP Lett. **21**, 80 (1975)].
- ³²R. N. Silver, Phys. Rev. [B] **11**, 1569 (1975).
- ³³V. S. Bagaev, N. V. Zamkovets, N. A. Penin, N. N. Sibel'din, and V. A. Tsvetkov, Zweite Intern. Tagung Laser und ihre Anwendungen, Dresden, DDR, 1973, k. 107; Prib. Tekh. Eksp. No. **2**, 258 (1974).

- ³⁴N. N. Sibel'din, V. S. Bagaev, V. A. Tsvetkov, and N. A. Penin, Preprint FIAN No. 117, Moscow, 1972.
- ³⁵N. N. Sibel'din, V. S. Bagaev, V. A. Tsvetkov, and N. A. Penin, Fiz. Tverd. Tela 15, 177 (1973) [Sov. Phys. Solid State 15, 121 (1973)].
- ³⁶Ya. E. Pokrovskii and K. I. Svistunova, Pis'ma Zh. Eksp. Teor. Fiz. 13, 297 (1971) [JETP Lett. 13, 201 (1971)].
- ³⁷R. N. Silver, Preprint, 1975.
- ³⁸R. W. Martin, Phys. Status Solidi [b] 61, 223 (1974).
- ³⁹Ya. E. Pokrovsky and K. I. Svistunova, Proc. Twelfth Intern. Conf. on Physics of Semiconductors, Stuttgart, 1974, p. 71.
- ⁴⁰Ya. E. Pokrovskii and K. I. Svistunova, Fiz. Tverd. Tela 16, 3399 (1974) [Sov. Phys. Solid State 16, 2202 (1975)].
- ⁴¹B. J. Feldman, Phys. Rev. Lett. 33, 359 (1974).
- ⁴²M. Voos, K. L. Shaklee, and J. M. Worlock, Phys. Rev. Lett. 33, 1161 (1974).
- ⁴³R. Becker and W. Döring, Ann. Phys. (Leipzig) 24, 719 (1935).
- ⁴⁴Ya. B. Zel'dovich, Zh. Eksp. Teor. Fiz. 12, 525 (1942).
- ⁴⁵Ya. I. Frenkel', Kineticheskaya teoriya zhidkostei (Kinetic Theory of Liquids), AN SSSR, 1945, Chap. VII.
- ⁴⁶V. S. Bagaev, L. V. Keldysh, N. N. Sibel'din, and V. A. Tsvetkov, Zh. Eksp. Teor. Fiz. 70, 702 (1976) [Sov. Phys. JETP 43, 362].
- ⁴⁷L. V. Keldysh, Pis'ma Zh. Eksp. Teor. Fiz. 23, 100 (1976) [JETP Lett. 23, 86 (1976)].

Translated by J. G. Adashko

Macroscopic theory of spin waves

A. F. Andreev and V. I. Marchenko

Physical Problems Institute, USSR Academy of Sciences

(Submitted November 17, 1975)

Zh. Eksp. Teor. Fiz. 70, 1522-1538 (April 1976)

A description of magnetic structures by means of macroscopic multipole moments is presented. All types of macroscopically distinct exchange magnetic structures are found for ferromagnets or collinear ferrimagnets (32 types), antiferromagnets (230 types), and noncollinear ferrimagnets (79 types). The general form of the equations that describe long-wave, low-frequency spin waves is elucidated. The examples considered show that in many cases there should exist anomalous branches of the spin oscillations.

PACS numbers: 75.30.Fv

The theory of spin waves is well developed for the case of ferromagnets. On the one hand, there is a microscopic approach^[1,2] that is based on the Heisenberg model and that enables us to explain the structure of the ground state of a ferromagnet and the spin-wave spectrum over the whole frequency range. On the other hand, the low-frequency, long-wave spin waves can be described macroscopically by means of the Landau-Lifshitz equation.^[3]

There is a completely different situation in the case of antiferromagnets. Here the microscopic problem can be solved only for spins that are large (i.e., quasi-classical), a property that they in fact, at least in the majority of cases, do not have. The existing phenomenological theory^[4,5] of low-frequency, long-wave spin-waves leads in many cases to satisfactory results. But this theory is essentially of model type, since the basic quantities of the theory (the sublattice moments) are not macroscopic. They cannot be obtained by macroscopic averaging of any physical quantities.

The present paper proposes a general macroscopic approach to the investigation of low-frequency, long-wave spin waves in any magnetic materials in which the magnetic ordering is the result of the action of exchange forces that appreciably exceed the relativistic interactions. The proposed approach uses no model-type concepts about the state of the magnetic material (localized spins, sublattices, etc.), but is essentially based only on symmetry considerations. The basic

quantities are macroscopic multipole moments, which are obtained from the true microscopic magnetic-moment density by a definite averaging over physically infinitesimal volumes.

The formulation of the macroscopic equations for spin waves is based to a significant degree on macroscopic analysis of the possible types of symmetry of exchange forces in magnetic materials. By means of multipole moments it proves possible to find all the types (their total number, as we shall see, is 373) of macroscopically different magnetic structures.

1. MACROSCOPIC MULTIPOLE MOMENTS

We shall first introduce the macroscopic multipole moments for the simplest case, in which they describe some scalar microscopic quantity. Let \mathcal{G} be the space group of the symmetry of the equilibrium state of the crystal: that is, the group of transformations with respect to which the equilibrium microscopic charge density is invariant. We consider some (in general nonequilibrium) state, described microscopically by a scalar quantity $f(\mathbf{r})$ (this may be, for example, the deviation of the charge density from its equilibrium value). The problem consists in finding the set of macroscopic quantities that describe this state as fully as is possible.

Any macroscopic quantity $F(\mathbf{r})$ must be obtained from $f(\mathbf{r})$ as a result of averaging over macroscopic volumes.